J Math Chem (2013) 51:1001–1022
DOI 10.1007/s10910-012-0129-0

ORIGINAL PAPER

Modelling interactions between a PBB and fullerenes

Ngamta Thamwattana · Thien Tran-Duc · Duangkamon Baowan

Received: 1 November 2012 / Accepted: 7 December 2012 / Published online: 24 December 2012

Abstract Fullerenes have many uses including in medical and electronic nanodevices. High pressure liquid chromatography (HPLC) columns are generally used to extract a certain structure of fullerne from a mixture of them. In this paper, we investigate the interactions between various types of fullerenes and a station phase in HPLC known as pentabromobenzyl (PBB). The Lennard-Jones potential and a continuum approach are employed to determine the van der Waals energy of these interactions within the HPLC columns. The equilibrium configurations for any given distance between a fullerene and the centre of a PBB are obtained. Results of this study may assist the design of a chromatography column for fullerene separation.

Keywords Fullerene · Pentabromobenzyl (PBB) · Separation · van der Waals interaction

N. Thamwattana
School of Mathematics and Applied Statistics,
University of Wollongong, Wollongong, NSW 2522, Australia

T. Tran-Duc
Department of Mechanical Engineering, Faculty of Engineering,
National University of Singapore, Singapore 119077, Singapore

D. Baowan (✉)
Department of Mathematics, Faculty of Science, Mahidol University,
Rama VI Rd., Bangkok 10400, Thailand
e-mail: duangkamon.bao@mahidol.ac.th

1 Introduction

The fullerene family, especially C_{60}, has appealing structural, electrochemical and physical properties, which can be exploited in various fields. For example, medical applications of fullerenes include antioxidant activity, antiviral activity and their use in drug delivery [1,15]. Another potential application of fullerenes is as containers for information-carrying spin systems for quantum computing. In particular, Harneit and co-workers [8,9] explore endohedral fullerenes $N@C_{60}$ and $P@C_{60}$ as quantum information carriers. For extensive details of various potential applications of fullerenes, we refer the reader to [5].

To employ fullerenes in many applications, it is required that single fullerene structures be extracted from a compound of carbon structures. Chromatography is the method for such separation. Generally, in a column chromatography, the mixture is dissolved in a fluid which is known as the mobile phase. The mobile phase is then passed through a column which contains a structure attached to another material called the stationary phase. The various constituents of fullerenes in the mixture travel at different velocities, causing them to separate. The separation is based on differential partitioning between the mobile and stationary phases. Differences in rates of movement through the stationary phase in the column give rise to different retention times of the fullerene molecules.

Commercially, the separation of fullerenes generally involves the use of high pressure liquid chromatography (HPLC). There are varieties of HPLC columns, which can separate different structures of fullerenes, including C_{60}, C_{70}, $C_{60} = O$ and endohedral fullerenes [10]. Stationary phases in the HPLC columns include pyrenylpropyl (buckyprep), phenothiazinyl (buckyprep-M) and pentabromobenzyl (PBB). PBBs are used as flame retardants and may be added to plastics to resolve their flammability. As an example, this paper models the interaction between various structures of fullerenes and a PBB. Understanding these interactions will enhance the performance of HPLC.

The HPLC is a basic laboratory procedure and can be used to determine the C_{60} : C_{70} ratio in a chemistry lab [16]. The endohedral fullerenes have been studied by a number of authors [4,11,12,14] who believe that the implanted atom will enhance the magnetic property of the system. Goedde et al. [7] use the HPLC technique to purify a mixture of $N@C_{60}$ and C_{60}. They observe that nitrogen atoms remain in the C_{60} during the process and maintain atomic configuration. Further, Suetsuna and co-workers [13] separate and identify $N_2@C_{60}$ and $N@C_{60}$ using HPLC. They report that their work was the first to show the existence of $N_2@C_{60}$ as endohedral C_{60} complex form.

As the interaction between fullerenes and PBBs is principally through van der Waals forces, it is appropriate to adopt the Lennard-Jones potential together with a continuum approach. In the continuum approach, atoms on a molecule are assumed to be uniformly distributed over its surface. As a result, the sum of all pair-wise interactions among atoms between two non-bonded molecules can be replaced by the double integral over the surfaces of the molecules multiplying by the atomic surface densities of each molecule. Through this technique, an analytical expression for the interaction energy between fullerenes and PBBs is obtained; these results can be used to elucidate the separation mechanisms within the HPLC columns. For more details of this approach we refer the reader to Girifalco et al. [6] and Cox et al. [2,3].

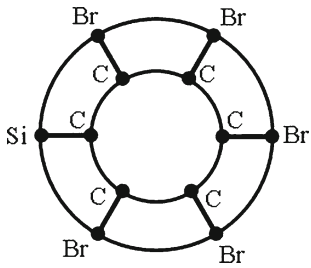

Fig. 1 Continuum model of a PBB molecule

This paper is structured as follows. In the following section, we detail the continuum models for a PBB and each of the fullerene structures. The interaction energy for the PBB and the fullerene structures are studied in Sect. 3. Numerical results for the four structures of fullerenes are presented in Sect. 4. Finally, the conclusions are given in Sect. 5. The mathematical derivations for the interaction energies between a point and a sphere, a point and a ring, a ring and a sphere and a point and an ellipsoid are presented in Appendices.

2 Continuum model for fullerene structures

In this section, we introduce a continuum approach in order to model the van der Waals interaction between a PBB and different types of fullerene structures.

A PBB molecule consists of six carbon atoms, five bromine atoms and one silicon atom. Each carbon atom is located at the vertex of a hexagonal lattice; the remaining atoms are connected to a carbon atom. Because the differences in bond lengths between Br-C and Si-C are very small, we assume in this model they are equal. Thus, a PBB molecule can be modelled as a combination of two concentric rings where atoms are uniformly distributed on each ring. The inner ring comprises carbon atoms and the outer ring is made up of bromine and silicon atoms, as depicted in Fig. 1. The atomic density for each ring is equal to the number of atoms divided by its circumference.

A C_{60} fullerene consists of sixty carbon atoms distributed over the surface of a sphere. In our model, we assume that carbon atoms are distributed uniformly over the surface of the sphere with an atomic surface density defined by the number of carbon atoms divided by the surface area of the sphere. A schematic model of the C_{60} fullerene is shown in Fig. 2a.

A $N@C_{60}$ molecule consists of a nitrogen atom located at the centre of a C_{60} fullerene. Here, we model a $N@C_{60}$ molecule as a sphere with a point located at its centre as shown in Fig. 2b. Again, we assume that sixty carbon atoms are uniformly distributed over the surface of the sphere.

A $C_{60} = O$ molecule comprises an oxygen atom connected to carbon atoms of a C_{60} fullerene via a double bond σ. Again we use a continuum model for the C_{60} molecule. Since we cannot determine exactly the position of the oxygen atom on the surface of the fullerene, we assume that the oxygen atom is located on the surface of an outer sphere, as shown in Fig. 2c, which has radius equal to the sum of the radius of the C_{60} fullerene and the bond length of C–O. In this study the bond length between a carbon and an oxygen atoms is taken to be 1.43 Å.

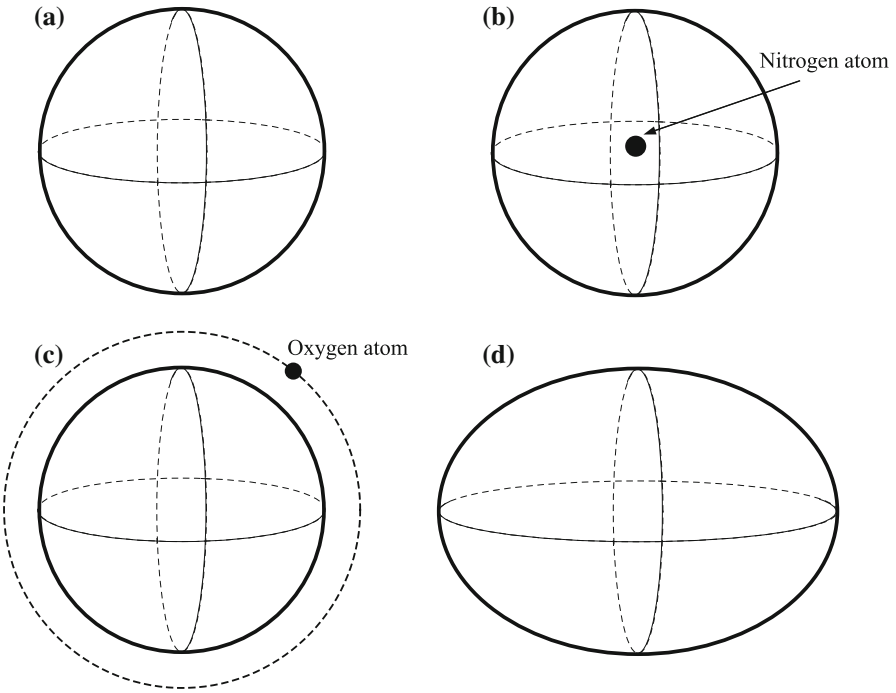

Fig. 2 Continuum models of **a** C_{60}, **b** $N@C_{60}$, **c** $C_{60} = O$ and **d** C_{70}

Table 1 Numerical values of radii and atomic densities

Radius of inner carbon ring on PBB	1.400	Å
Radius of outer Br-Si ring on PBB	3.340	Å
Radius of C_{60} fullerene	3.55	Å
Radius of oxygen sphere on $C_{60} = O$	4.98	Å
C_{70} equatorial semi-axis length	3.59	Å
C_{70} polar semi-axis length	4.17	Å
Atomic line density of inner carbon ring on PBB	0.682	$Å^{-1}$
Atomic line density of outer Br-Si ring on PBB	0.286	$Å^{-1}$
Atomic surface density of C_{60}	0.379	$Å^{-2}$
Atomic surface density of oxygen sphere on $C_{60} = O$	0.00321	$Å^{-2}$
Atomic surface density of C_{70}	0.3896	$Å^{-2}$

Finally, a C_{70} molecule can be modelled as a spheroid (i.e. an ellipsoid with two equal major axes) and carbon atoms are assumed to be uniformly distributed over its surface as depicted in Fig. 2d.

Values of radii and atomic densities for these molecules are given in Table 1.

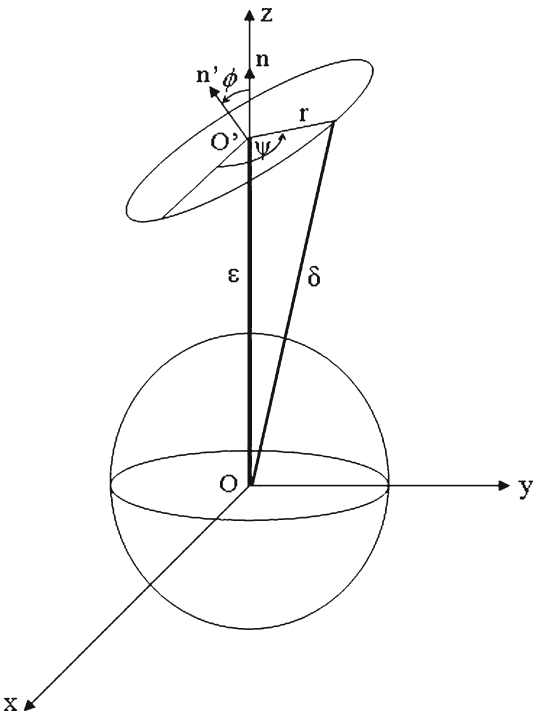

Fig. 3 Model for the interaction between a *ring* and a *sphere*

3 Interactions between a PBB and fullerenes

3.1 PBB and C_{60} fullerene

As mentioned in Sect. 2, a PBB molecule is modelled as a combination of a carbon ring and a bromine-silicon ring, and a C_{60} molecule is modelled as a sphere, thus the interaction energy between a PBB and a C_{60} fullerene can be obtained from the sum of the interactions between the two rings and the C_{60} molecule, namely

$$E_{PBB-C_{60}} = E_{C-C_{60}} + E_{BrSi-C_{60}}. \tag{1}$$

The schematic illustration for the model of the interaction between a ring and a sphere is presented in Fig. 3. In Fig. 3, we use a rotational angle ϕ and a distance between the two centres ε to describe the relative positions of the ring and the sphere.

Assuming a continuum approach the interaction energy between a ring and a sphere is given by

$$E_{ring-sphere} = \eta_{ring}\eta_{sphere} \int_C \int_S V(\rho) dS d\ell, \tag{2}$$

where η_{ring} and η_{sphere} are the line density of a ring and the surface density of the sphere, respectively, $V(\rho)$ is a potential function and here we adopt the Lennard-Jones

Table 2 Lennard-Jones parameters

Atom	ϵ (kcal/mol)	σ (Å)
C	0.0951	3.473
Br	0.3700	3.519
Si	0.3100	3.804
N	0.0774	3.263
O	0.0957	3.033

potential which is given by

$$V(\rho) = -\frac{A}{\rho^6} + \frac{B}{\rho^{12}}, \tag{3}$$

where ρ is Euclidean distance between a line element $d\ell$ on the ring and a surface element dS on the spherical surface, $A = 4\epsilon\sigma^6$ and $B = 4\epsilon\sigma^{12}$ are the attractive and the repulsive constants, respectively. Values of the well depth ϵ and the van der Waals diameter σ for various types of atoms used in this paper are given in Table 2. The Lennard-Jones parameters (ϵ and σ) are originally defined for the interaction between two atoms of the same kind. For interactions between two atoms of different kinds, ϵ and σ are calculated using Lorentz-Berthelot mixing rules, namely $\epsilon_{XY} = (\epsilon_X \epsilon_Y)^{1/2}$ and $\sigma_{XY} = (\sigma_X + \sigma_Y)/2$. We note that for the interaction between the Br-Si ring and the C_{60} molecule, the attractive and the repulsive constants are calculated based on the portion of contribution from bromine and silicon atoms in the Br-Si ring. As such we have

$$A = \frac{5A_{Br-C} + A_{Si-C}}{6}, \quad B = \frac{5B_{Br-C} + B_{Si-C}}{6}. \tag{4}$$

In Appendix C, we obtain an analytical expression (18) for the interaction energy of a C_{60} fullerene and a PBB system. At a given distance between the two centres of the PBB and the C_{60} fullerene, the equilibrium configuration of the two molecules can be determined by minimizing the interaction energy between them. As the distance varies, the equilibrium configuration changes. All possible equilibrium configurations for a PBB interacting with a C_{60} molecule are shown in Fig. 4.

3.2 PBB and N@C_{60}

The interaction between a PBB and a N@C_{60} can be found from the sum of the interactions of the PBB with the C_{60} fullerene and the nitrogen atom,

$$E_{PBB-N@C_{60}} = E_{PBB-C_{60}} + E_{PBB-N}. \tag{5}$$

The interaction energy between the PBB and the fullerene C_{60} ($E_{PBB-C_{60}}$) is as shown in Sect. 3.1, while the interaction between the PBB and the nitrogen atom can

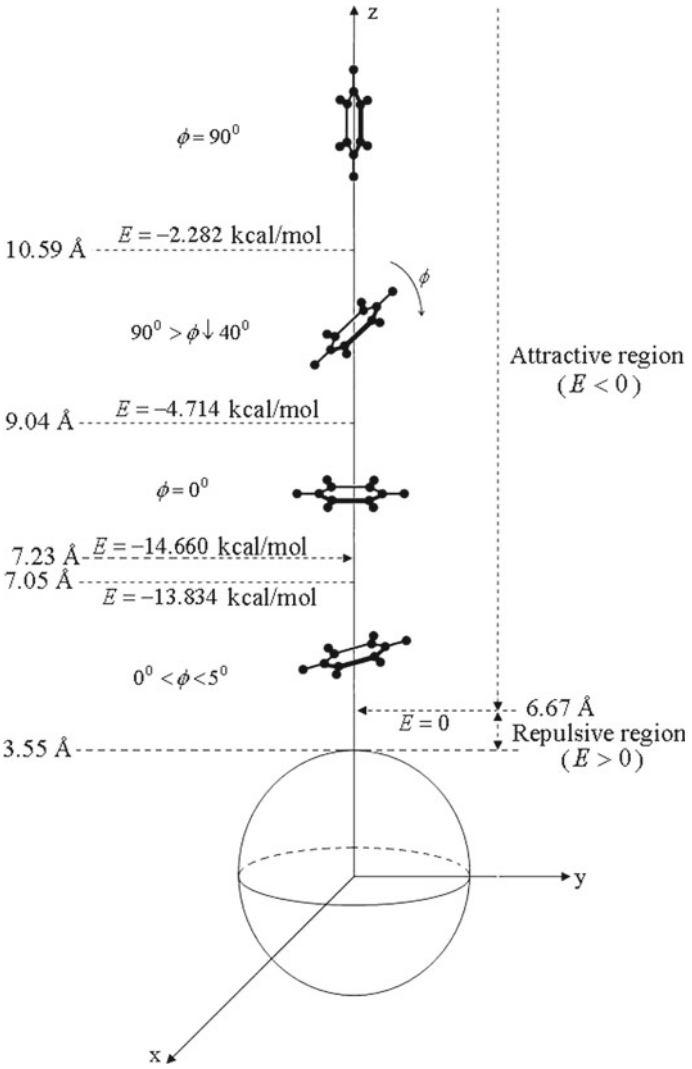

Fig. 4 Equilibrium configurations and corresponding local minimum energies for a PBB molecule interacting with a C_{60} fullerene as the distance between the two centres varies

be calculated as the sum of two interactions, namely carbon ring–nitrogen atom and bromine-silicon ring–nitrogen atom. Thus we have

$$E_{PBB-N} = E_{C-N} + E_{BrSi-N}. \tag{6}$$

The interaction energy between an atom and a ring is given by

$$E_{atom-ring} = \eta_{ring} \int_C V(\rho) d\ell, \tag{7}$$

where $V(\rho)$ is the Lennard-Jones potential and ρ is the distance between the atom and a line element $d\ell$ of the ring. The mathematical derivation for the interaction between an atom and a ring is given in Appendix B. We note that the relative positions of the nitrogen atom and the ring can also be described by the same pair of parameters ε and ϕ as shown in Sect. 3.1 because the nitrogen atom is assumed to be located at the centre of the sphere. The attractive and the repulsive constants for the interaction between Br-Si ring and N can be calculated similarly to those of Br-Si ring and C_{60} sphere Eq. (4). Using (16) for E_{PBB-N} and substituting (27) for $n = 3$ and 6 into (18) for $E_{PBB-C_{60}}$, and varying the distance between the two centres ε, all possible equilibrium configurations of a PBB interacting with a N@C_{60} are given in Fig. 5.

3.3 PBB and $C_{60} = O$

The total interaction between a PBB and a $C_{60} = O$ can be derived from the sum of two interactions of the PBB with the inner and outer spheres, (i.e. C_{60} and oxygen sphere). As a result we have

$$E_{PBB-C_{60}=O} = E_{PBB-C_{60}} + E_{PBB-O}. \tag{8}$$

Because the oxygen atom is assumed to be located on the outer spherical surface, the energy E_{PBB-O} can be obtained by summing up the two interactions between carbon and bromine-silicon rings and the oxygen sphere. Again, the attractive and repulsive constants for the interaction between Br-Si ring and oxygen sphere can be calculated similarly to those of Br-Si ring and C_{60} sphere Eq. (4).

From (18) and (8), we determine all possible equilibrium configurations for the interaction of a PBB and a $C_{60} = O$ depending on the distance between the two centres (see Fig. 6).

3.4 PBB and C_{70}

In this case, the total interaction energy can be obtained from the sum of the two interactions of carbon and bromine-silicon rings with the ellipsoidal fullerene C_{70}. The schematic illustration for the interaction between a ring and an ellipsoid is given in Fig. 7. Here, we use three rotational angles (ϕ, θ and ζ) and a distance between the two centres ε to describe relative positions of a ring and an ellipsoid.

In Appendix D, the total interaction energy of this system is obtained analytically. Using (28) all possible equilibrium configurations of a PBB and a C_{70} fullerene as the distance between the two centres varies are illustrated in Fig. 8. We note that when distance between the two centres is greater than or equal to 7.16 Å, the equilibrium configurations are obtained at $\zeta = \theta = 0$. Further, when ε is less than 7.16 Å, equilibrium configurations are obtained at $\zeta = \pi/2$ and $\phi = 0$.

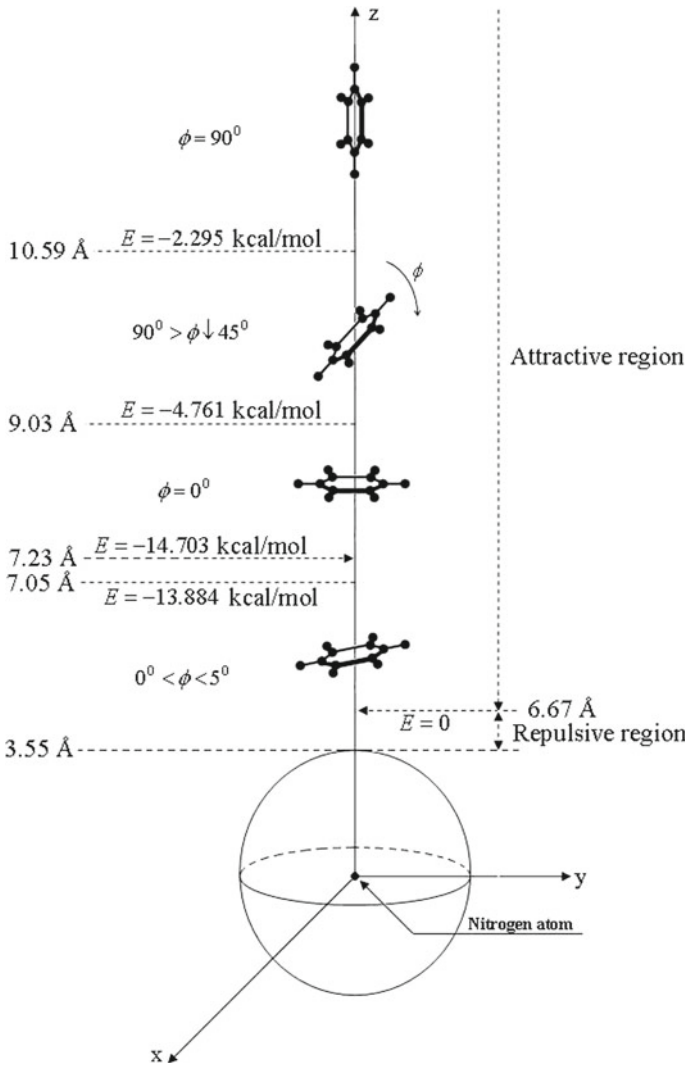

Fig. 5 Equilibrium configurations and corresponding local minimum energies for a PBB molecule interacting with a $N@C_{60}$ structure as the distance between the two centres varies

4 Results and discussion

The Lennard-Jones potential function and the continuum approach are employed to determine the van der Waals interactions between a PBB and various types of fullerene structures. In the cases of the interactions between a PBB and symmetric fullerenes, namely C_{60}, $N@C_{60}$ and $C_{60} = O$, the global minimum energies occur at the distances 7.23, 7.23 and 7.48 Å, respectively, above the fullerene centres where the rotational angle ϕ of the PBB is zero. These positions correspond to the energies of -14.660, -14.703 and -12.588 kcal/mol, respectively. Moreover, for any given

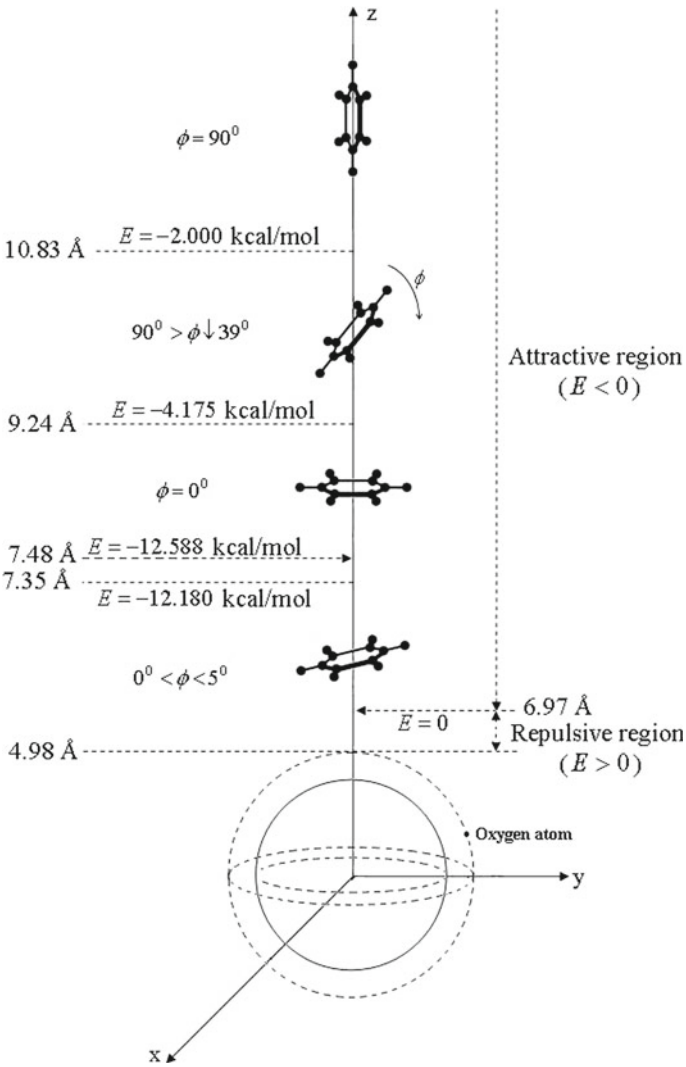

Fig. 6 Equilibrium configurations and corresponding local minimum energies for a PBB molecule interacting with a $C_{60} = O$ structure as the distance between the two centres varies

rotational angle ϕ and the distances between a PBB and a fullerene centres, the equilibrium location can be determined as shown in Figs. 4, 5, 6 and 8.

We observe similar behaviours for the systems of C_{60} and $N@C_{60}$. This is due to the fact that there is only one nitrogen atom in the latter case which makes only a small contribution of the van der Waals interaction to the system. On the other hand, a sphere of oxygen atom in the case of $C_{60} = O$ plays a major role in the determination of the interaction energy, as such we obtain slightly lower minimum energy.

In the system of a PBB interacting with a C_{70}, we consider both the interactions in the equatorial semi-axis and the polar semi-axis. In the equatorial direction, the PBB ring is

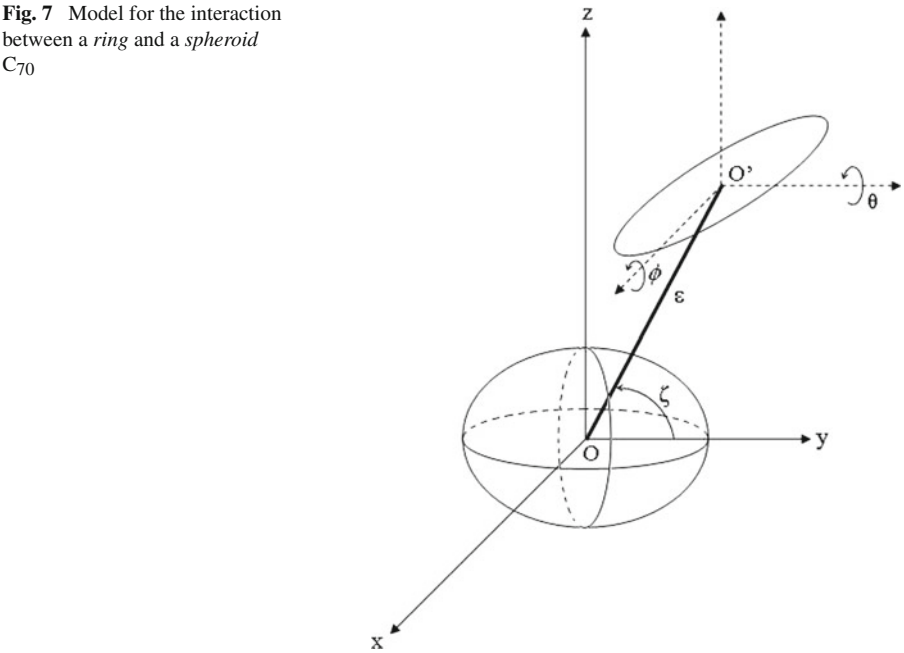

Fig. 7 Model for the interaction between a *ring* and a *spheroid* C_{70}

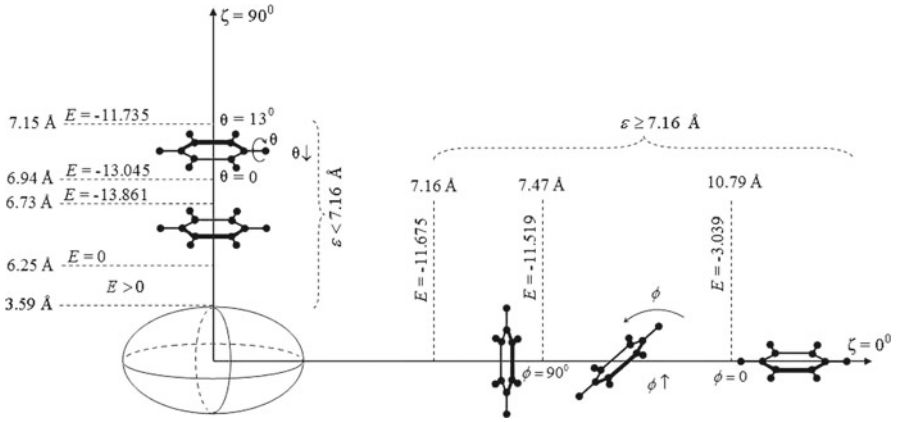

Fig. 8 Equilibrium configurations and corresponding local minimum energies for a PBB molecule interacting with a C_{70} fullerene as the distance between the two centres varies

likely to locate parallel to the C_{70} surface with $\phi = 0$. Once the distance from the centre of the C_{70} to the PBB is greater than 6.25 Å, the system is energetically favourable, and the global minimum energy occurs at the distance 6.73 Å corresponding to the energy -13.861 kcal/mol. In terms of the polar direction, we observe various configurations of PBB, as shown in Fig. 8. However, the most stable configuration occurs when the PBB is parallel to the C_{70} surface in the polar semi-axis with the distance 7.16 Å from the centre of the C_{70} and the corresponding energy is -11.675 kcal/mol. The summary of the global minimum energy and the equilibrium distance for the four types of fullerenes are presented in Table 3.

Table 3 Global minimum energy and equilibrium distance for different types of interactions

Interactions	Global minimum energy (kcal/mol)	Equilibrium distance (Å)
PBB–C_{60}	−14.660	7.23
PBB–N@C_{60}	−14.703	7.23
PBB–C_{60} = O	−12.588	7.48
PBB–C_{70}	−13.861	6.73 (in equatorial direction)

5 Conclusions

In this paper, we mathematically model the interactions between a PBB and various types of fullerene structures, which are C_{60}, N@C_{60}, C_{60} = O and C_{70}, using a continuum approach and the Lennard-Jones potential. For each interaction depending on the distance between the centres of the PBB and the fullerene structure, we obtain all possible equilibrium configurations and the corresponding energies. This finding may be used to improve the design of the high pressure liquid chromatography columns to purify the mixture of fullerenes.

Acknowledgments The authors acknowledge financial support from the Faculty of Informatics, University of Wollongong (UOW) and UOW's Internationalisation Linkage Grant Scheme.

6 Appendix A: Interaction energy between a point and a sphere

In this appendix, we derive analytical expressions for the interaction energy between a point and a sphere. A point is assumed to be located at a distance δ from the centre of the sphere where $\delta > R$ and R denotes the radius of the sphere. The origin is assumed to be located at the centre of the sphere, and the schematic diagram of the coordinate system of this problem is as shown in Fig. 9. The interaction energy between the point and the spherical fullerene is then given by

$$E_{point-sphere} = \eta_{sphere} \int_0^{\pi} \int_0^{2\pi} \left(-\frac{A}{\rho_\delta^6} + \frac{B}{\rho_\delta^{12}} \right) R^2 \sin\gamma \, d\zeta \, d\gamma, \tag{9}$$

where ρ_δ is a distance from a surface element of the sphere which is given by $\rho_\delta^2 = R^2 + \delta^2 - 2\delta R\cos\gamma$. The parameter η_{sphere} represents the mean atomic surface density of the sphere, and A and B are the Lennard-Jones constants. For convenience, we rewrite (9) in terms of

$$J_n = \int_0^{\pi} \int_0^{2\pi} R^2 \sin\gamma \rho_\delta^{-2n} d\zeta \, d\gamma, \qquad n = 3, 6, \tag{10}$$

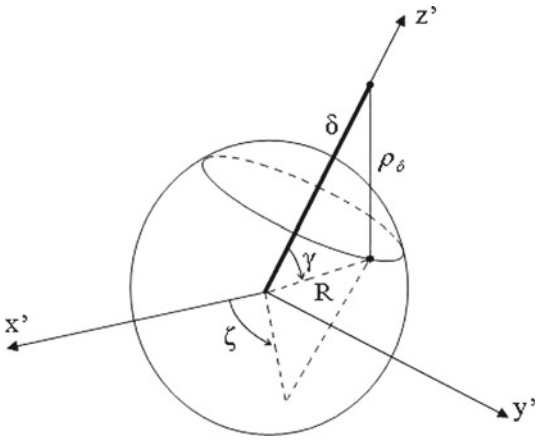

Fig. 9 Model for the interaction between a point and a *sphere*

to give

$$E_{point-sphere} = \eta_{sphere}(-AJ_3 + BJ_6). \tag{11}$$

It can be shown that (10) is independent of ζ, and we may deduce

$$J_n = 2\pi R^2 \int_0^\pi \frac{\sin\gamma}{(R^2+\delta^2-2\delta R\cos\gamma)^n} d\gamma.$$

On substituting $t = R^2 + \delta^2 - 2\delta R\cos\gamma$ and integrating, we obtain

$$J_n = \frac{\pi R}{\delta(n-1)}\left[\frac{1}{(\delta-R)^{2(n-1)}} - \frac{1}{(\delta+R)^{2(n-1)}}\right]. \tag{12}$$

Therefore, the interaction energy between a point and a spherical fullerene is given by

$$E_{point-sphere} = \eta_{sphere}\frac{\pi R}{\delta}\left\{-\frac{A}{2}\left[\frac{1}{(\delta-R)^4} - \frac{1}{(\delta+R)^4}\right] + \frac{B}{5}\left[\frac{1}{(\delta-R)^{10}} - \frac{1}{(\delta+R)^{10}}\right]\right\}. \tag{13}$$

7 Appendix B: Interaction energy between a point and a ring

Here, we consider the interaction energy between a point (or an atom) and a ring. On using the Lennard-Jones potential function and the continuum approximation for a line integral of the ring, the interaction energy of the system can be written as

$$E_{point-ring} = \eta_{ring} \int_0^{2\pi} r \left(\frac{-A}{\delta^6} + \frac{B}{\delta^{12}} \right) d\psi, \tag{14}$$

where δ is the distance between a line element on the ring and the atom,

$$\delta^2 = r^2 + \epsilon^2 + 2r\epsilon \sin\phi \sin\psi. \tag{15}$$

Here r is the radius of the ring, and η_{ring} is the mean atomic line density of the ring. The Cartesian coordinates of the ring is as presented in Fig. 3. For convenience, we write

$$E_{point-ring} = \eta_{ring}(-AK_3 + BK_6),$$

where

$$\begin{aligned} K_n &= r \int_0^{2\pi} \delta^{-2n} d\psi = r \int_0^{2\pi} \frac{1}{(r^2 + \epsilon^2 + 2r\epsilon \sin\phi \sin\psi)^n} d\psi \\ &= r \int_0^{2\pi} \frac{1}{(r^2 + \epsilon^2 + 2r\epsilon \sin\phi \cos\psi)^n} d\psi \\ &= r \int_0^{2\pi} \frac{1}{[r^2 + \epsilon^2 + 2r\epsilon \sin\phi - 4r\epsilon \sin\phi \sin^2(\psi/2)]^n} d\psi, \qquad n = 3, 6. \end{aligned}$$

Note that we have interchanged $\sin\psi$ and $\cos\psi$ using the fact that they are periodic functions with a period of 2π. On substituting $t = \sin^2(\psi/2)$, we have

$$\begin{aligned} K_n &= 2r \int_0^1 \frac{t^{-1/2}(1-t)^{-1/2}}{(r^2 + \epsilon^2 + 2r\epsilon \sin\phi - 4r\epsilon t \sin\phi)^n} dt, \\ &= \frac{2r}{(r^2 + \epsilon^2 + 2r\epsilon \sin\phi)^n} \int_0^1 \frac{t^{-1/2}(1-t)^{-1/2}}{(1-\mu t)^n} dt, \end{aligned}$$

where $\mu = 4r\epsilon \sin\phi/(r^2 + \epsilon^2 + 2r\epsilon \sin\phi)$. Therefore, we may write K_n in terms of a hypergeometric function,

$$K_n = \frac{2\pi r}{(r^2 + \epsilon^2 + 2r\epsilon \sin\phi)^n} F(n, 1/2; 1; \mu).$$

The interaction energy between a point and a ring is then given by

$$E_{point-ring} = 2\pi r\eta_{ring}\left\{-\frac{A}{(r^2+\epsilon^2+2r\epsilon\sin\phi)^3}F(3,1/2;1;\mu) + \frac{B}{(r^2+\epsilon^2+2r\epsilon\sin\phi)^6}F(6,1/2;1;\mu)\right\}. \quad (16)$$

8 Appendix C: Interaction energy between a ring and a sphere

Assuming that an atom defined in Appendix A is located on a ring, the interaction energy between a ring and a spherical fullerene can be obtained by evaluating another line integral of $E_{point-sphere}$. Then we have

$$E_{ring-sphere} = r\eta_{ring}\int_0^{2\pi} E_{point-sphere}(\psi)d\psi, \quad (17)$$

where $E_{point-sphere}$ is defined by (9), again r denotes the radius of the ring and η_{ring} is the mean atomic line density of the ring. On substituting (11) and (12) into (17), we have

$$E_{ring-sphere} = \eta_{ring}\eta_{sphere}(-AI_3 + BI_6), \quad (18)$$

where

$$I_n = \frac{\pi rR}{(n-1)}\int_0^{2\pi}\frac{1}{\delta}\left[\frac{1}{(\delta-R)^{2(n-1)}} - \frac{1}{(\delta+R)^{2(n-1)}}\right]d\psi, \qquad n = 3, 6. \quad (19)$$

Equation (19) can be rewritten as

$$I_n = \frac{\pi rR}{(n-1)}\int_0^{2\pi}\frac{1}{\delta}\frac{(\delta+R)^{2(n-1)} - (\delta-R)^{2(n-1)}}{(\delta^2-R^2)^{2(n-1)}}d\psi. \quad (20)$$

On expanding the numerator in (20), we obtain

$$I_n = \frac{2\pi rR}{(n-1)}\sum_{k=0}^{n-2}\frac{(2n-2)!R^{2n-2k-3}}{(2n-2k-3)!(2k+1)!}H_{nk}, \quad (21)$$

where

$$H_{nk} = \int_0^{2\pi} \frac{\delta^{2k}}{(\delta^2 - R^2)^{2(n-1)}} d\psi. \tag{22}$$

On substituting the expression of δ defined by (15) into (22), we obtain

$$H_{nk} = \int_0^{2\pi} \frac{(r^2 + \epsilon^2 + 2\epsilon r \sin\phi \sin\psi)^k}{(r^2 + \epsilon^2 + 2\epsilon r \sin\phi \sin\psi - R^2)^{2(n-1)}} d\psi. \tag{23}$$

Since the integrand in (23) is a periodic function with the period of 2π, then $\cos\psi$ and $\sin\psi$ are interchangeable. Therefore,

$$H_{nk} = \int_0^{2\pi} \frac{(r^2 + \epsilon^2 + 2\epsilon r \sin\phi \cos\psi)^k}{(r^2 + \epsilon^2 + 2\epsilon r \sin\phi \cos\psi - R^2)^{2(n-1)}} d\psi. \tag{24}$$

Next, we use the trigonometric identity $\cos\psi = 1 - 2\sin^2(\psi/2)$, expanding the numerator in (24) in terms of $\sin^2(\psi/2)$ to obtain

$$H_{nk} = \sum_{m=0}^{k} \frac{k!(r^2 + \epsilon^2 + 2\epsilon r \sin\phi)^m (-4\epsilon r \sin\phi)^{k-m}}{(k-m)!m!} \times \int_0^{2\pi} \frac{\sin^{2k-2m}(\psi/2)}{\left[r^2 + \epsilon^2 + 2\epsilon r \sin\phi - 4\epsilon r \sin\phi \sin^2(\psi/2) - R^2\right]^{2(n-1)}} d\psi.$$

On substituting $t = \sin^2(\psi/2)$, we have

$$H_{nk} = \sum_{m=0}^{k} \frac{k!(r^2 + \epsilon^2 + 2\epsilon r \sin\phi)^m (-4\epsilon r \sin\phi)^{k-m}}{(k-m)!m!(r^2 + \epsilon^2 + 2\epsilon r \sin\phi - R^2)^{2n-2}} \times 2 \int_0^1 \frac{t^{2k-2m-1/2}(1-t)^{-1/2}}{(1-\mu t)^{2(n-1)}} dt, \tag{25}$$

where in this case $\mu = 4\epsilon r \sin\phi/(r^2 + \epsilon^2 + 2\epsilon r \sin\phi - R^2)$. The Eq. (25) can be written in terms of hypergeometric functions,

$$H_{nk} = \sum_{m=0}^{k} \frac{k!(r^2 + \epsilon^2 + 2\epsilon r \sin\phi)^m (-4\epsilon r \sin\phi)^{k-m}}{(k-m)!m!(r^2 + \epsilon^2 + 2\epsilon r \sin\phi - R^2)^{2n-2}} \times \frac{2\pi^{1/2}}{(2k - 2m + 1/2)} F(2n-2, 2k-2m+1/2; 2k-2m+3/2; \mu). \tag{26}$$

On substituting (26) into (21), we obtain the final form of I_n as follows

$$I_n = \frac{4\pi^{3/2} r R}{(1-n)} \sum_{k=0}^{n-2} \frac{(2n-2)! R^{2n-2k-3}}{(2n-2k-3)!(2k+1)!} \times \sum_{m=0}^{k} \frac{k!(r^2+\epsilon^2+2\epsilon r\sin\phi)^m(-4\epsilon r\sin\phi)^{k-m}}{(k-m)!m!(r^2+\epsilon^2+2\epsilon r\sin\phi-R^2)^{2n-2}(2k-2m+1/2)} \times F(2n-2, 2k-2m+1/2; 2k-2m+3/2; \mu). \quad (27)$$

The interaction energy between a ring and a sphere can be obtained by substituting I_n defined by (27) for $n = 3$ and 6 into (18).

9 Appendix D: Interaction energy between a ring and an ellipsoid

In Cartesian coordinate system, an arbitrary point on the ellipsoid has coordinates $(a\sin\gamma\cos\eta, b\cos\gamma, a\sin\gamma\sin\eta)$, and an arbitrary point on the ring has coordinates (X, Y, Z) where

$$\begin{aligned} X &= r\cos\psi\cos\theta - r\sin\psi\sin\phi\sin\theta, \\ Y &= r\sin\psi\cos\phi + \epsilon\cos\zeta, \\ Z &= r\cos\psi\sin\theta + r\sin\psi\sin\phi\cos\theta + \epsilon\sin\zeta. \end{aligned}$$

The schematic model for a system of a ring and an ellipsoid is depicted in Fig. 7. The distance between an arbitrary point on the ring and an arbitrary point on then surface of the ellipsoid is then given by

$$\begin{aligned} \rho^2 &= (a\sin\gamma\cos\eta - X)^2 + (b\cos\gamma - Y)^2 + (a\sin\gamma\sin\eta - Z)^2 \\ &= K_1 + K_2\cos(\eta - \eta_0), \end{aligned}$$

where $K_1 = a^2\sin^2\gamma + X^2 + (b\cos\gamma - Y)^2 + Z^2$, $K_2 = 2a\sin\gamma(X^2+Z^2)^{1/2}$ and $\eta_0 = \arctan(Z/X)$. On using the Lennard-Jones potential function and the continuum approximation, the interaction energy between the ring and the ellipsoid of C_{70} is

$$E_{ring-ellipsoid} = \eta_{ring}\eta_{ellipsoid}\int_{\ell}\int_{S}\left(-\frac{A}{\rho^6} + \frac{B}{\rho^{12}}\right)dSd\ell,$$

where dS is the surface area element of the ellipsoid and $d\ell$ denotes the arc length element of a line integral of the ring. For convenience, we write

$$E_{ring-ellipsoid} = \eta_{ring}\eta_{ellipsoid}(-AJ_3 + BJ_6), \quad (28)$$

where

$$J_n = \int_{\ell} \int_{S} \frac{1}{\rho^{2n}} dS d\ell.$$

Upon parameterising, the integral J_n becomes

$$\begin{aligned} J_n &= ar \int_0^{\pi} \int_0^{2\pi} \int_0^{2\pi} \frac{1}{\rho^{2n}} \sin\gamma \sqrt{a^2\cos^2\gamma + b^2\sin^2\gamma}\, d\eta d\psi d\gamma, \\ &= ar \int_0^{\pi} \int_0^{2\pi} \sin\gamma \sqrt{a^2\cos^2\gamma + b^2\sin^2\gamma}\, I_n d\psi d\gamma, \end{aligned} \tag{29}$$

where

$$I_n = \int_0^{2\pi} \frac{1}{[K_1 + K_2\cos(\eta - \eta_0)]^n} d\eta.$$

Since $\cos(\eta - \eta_0)$ has period 2π,

$$I_n = \int_0^{2\pi} \frac{1}{(K_1 + K_2\cos\eta)^n} d\eta.$$

On substituting $t = \sin^2(\eta/2)$, we have

$$I_n = 2\int_0^1 \frac{t^{-1/2}(1-t)^{-1/2}}{(K_1 + K_2 - 2K_2 t)^n} dt.$$

We can write the above integral in terms of a hypergeometric function,

$$I_n = \frac{2\pi}{(K_1 + K_2)^n} F\left(n, \frac{1}{2}; 1; \frac{2K_2}{K_1 + K_2}\right).$$

Since

$$F(a, b; 2b; z) = (1 - z/2)^{-a} F\left(\frac{a}{2}, \frac{a}{2} + \frac{1}{2}; b + \frac{1}{2}; \left(\frac{z}{(2-z)}\right)^2\right),$$

we have

$$I_n = \frac{2\pi}{K_1^n} F\left(\frac{n}{2}, \frac{n}{2} + \frac{1}{2}; 1; \frac{K_2^2}{K_1^2}\right). \tag{30}$$

We substitute (30) into (29) and then expand the hypergeometric function to obtain

$$J_n = 2\pi ar \sum_{i=0}^{\infty} \frac{\left(\frac{n}{2}\right)_i \left(\frac{n}{2} + \frac{1}{2}\right)_i}{i!^2} \int_0^{\pi} \sin\gamma \sqrt{a^2 \cos^2\gamma + b^2 \sin^2\gamma}\, H_{ni} d\gamma,$$

where

$$H_{ni} = \int_0^{2\pi} \frac{K_2^{2i}}{K_1^{n+2i}} d\psi.$$

Next, we may write expressions of K_1 and K_2 in terms of $\sin\psi$ and $\cos\psi$ to obtain

$$\begin{aligned} K_1 &= \alpha_1 + \sqrt{\alpha_2^2 + \alpha_3^2}\cos(\psi - \psi_0), \\ K_2 &= (2a\sin\gamma)^{2i}(\alpha_4 + \alpha_5\cos^2\psi + \alpha_2\cos\psi + \alpha_6\sin\psi), \end{aligned}$$

where

$$\begin{aligned} \alpha_1 &= a^2\sin^2\gamma + b^2\cos^2\gamma + r^2 + \epsilon^2 - 2b\epsilon\cos\gamma\cos\zeta, \\ \alpha_2 &= 2\epsilon r\sin\theta\sin\zeta, \\ \alpha_3 &= 2r(\epsilon\cos\phi\cos\zeta + \epsilon\sin\phi\cos\theta\sin\zeta - b\cos\gamma\cos\phi), \\ \alpha_4 &= r^2\sin^2\phi + \epsilon^2\sin^2\zeta, \\ \alpha_5 &= r^2\cos^2\phi, \\ \alpha_6 &= 2\epsilon r\sin\phi\cos\theta\sin\zeta, \\ \psi_0 &= \arctan(\alpha_3/\alpha_2). \end{aligned}$$

Therefore,

$$H_{ni} = (2a\sin\gamma)^{2i} \int_0^{2\pi} \frac{(\alpha_4 + \alpha_5\cos^2\psi + \alpha_2\cos\psi + \alpha_6\sin\psi)^i}{\left[\alpha_1 + \sqrt{\alpha_2^2 + \alpha_3^2}\cos(\psi - \psi_0)\right]^{n+2i}} d\psi.$$

Again since $\cos(\psi - \psi_0)$ has period 2π, we can replace ψ by $\psi + \psi_0$, so we have

$$H_{ni} = (2a\sin\gamma)^{2i}\int_0^{2\pi}\frac{[\alpha_4+\alpha_5\cos^2(\psi+\psi_0)+\alpha_2\cos(\psi+\psi_0)+\alpha_6\sin(\psi+\psi_0)]^i}{(\alpha_1+\sqrt{\alpha_2^2+\alpha_3^2}\cos\psi)^{n+2i}}d\psi. \tag{31}$$

On rearranging the numerator of (31) in terms of ψ, we have

$$H_{ni}=(2a\sin\gamma)^{2i}\int_0^{2\pi}\frac{(\beta_1+\beta_2\cos^2\psi+\beta_3\sin\psi\cos\psi+\beta_4\sin\psi+\beta_5\cos\psi)^i}{(\alpha_1+\sqrt{\alpha_2^2+\alpha_3^2}\cos\psi)^{n+2i}}d\psi, \tag{32}$$

where $\beta_1 = \alpha_4+\alpha_5\sin^2\psi_0$, $\beta_2 = \alpha_5\cos(2\psi)$, $\beta_3 = -\alpha_5\sin(2\psi_0)$, $\beta_4=-\alpha_2\sin\psi_0+\alpha_6\cos\psi_0$ and $\beta_5=\alpha_2\cos\psi_0+\alpha_6\sin\psi_0$. Then, equation for H_{ni} becomes

$$H_{ni} = (2a\sin\gamma)^{2i}\sum_{k=0}^{i}\sum_{m=0}^{k}\sum_{p=0}^{m}\sum_{q=0}^{p}\frac{i!\beta_1^{i-k}\beta_2^{k-m}\beta_3^{m-p}\beta_4^{q}\beta_5^{p-q}}{(i-k)!(k-m)!(m-p)!(p-q)!q!}$$
$$\times\int_0^{2\pi}\frac{\cos^{2k-m-q}\psi\sin^{m-p+q}\psi}{(\alpha_1+\sqrt{\alpha_2^2+\alpha_3^2}\cos\psi)^{n+2i}}d\psi.$$

On substituting $u=\sin^2(\psi/2)$, we have

$$H_{ni} = (2a\sin\gamma)^{2i}\sum_{k=0}^{i}\sum_{m=0}^{k}\sum_{p=0}^{m}\sum_{q=0}^{p}\frac{i!\beta_1^{i-k}\beta_2^{k-m}\beta_3^{m-p}\beta_4^{q}\beta_5^{p-q}}{(i-k)!(k-m)!(m-p)!(p-q)!q!}$$
$$\times\sum_{s=0}^{2k-m-q}\frac{(-1)^s2^{2m-p+q+s}(2k-m-q)!}{(2k-m-q-s)!s!(\alpha_1+\sqrt{\alpha_2^2+\alpha_3^2})^{n+2i}}$$
$$\times\int_0^1\frac{u^{(m-p+q+2s-1)/2}(1-u)^{(m-p+q-1)/2}}{(1-\nu t)^{n+2i}}du,$$

where $\nu=2\sqrt{\alpha_2^2+\alpha_3^2}/(\alpha_1+\sqrt{\alpha_2^2+\alpha_3^2})$, and therefore, we may write this equation in terms of the hypergeometric function

$$H_{ni} = (2a\sin\gamma)^{2i}\sum_{k=0}^{i}\sum_{m=0}^{k}\sum_{p=0}^{m}\sum_{q=0}^{p}\frac{i!\beta_1^{i-k}\beta_2^{k-m}\beta_3^{m-p}\beta_4^{q}\beta_5^{p-q}}{(i-k)!(k-m)!(m-p)!(p-q)!q!}$$
$$\times\sum_{s=0}^{2k-m-q}\frac{(-1)^s 2^{2m-p+q+s}(2k-m-q)!}{(2k-m-q-s)!s!(\alpha_1+\sqrt{\alpha_2^2+\alpha_3^2})^{n+2i}}$$
$$\times\frac{\Gamma(w/2+s)\Gamma(w/2)}{\Gamma(w+s)}F(n+2i, w/2+s; w+s; \nu),$$

where $w = m - p + q + 1$. Now, we use the relation $F(a, b; c; z) = (1-z)^{-b}F(b, c-a; c; z(z-1)^{-1})$ to terminate the hypergeometric series, and we may deduce

$$H_{ni} = (2a\sin\gamma)^{2i}\sum_{k=0}^{i}\sum_{m=0}^{k}\sum_{p=0}^{m}\sum_{q=0}^{p}\frac{i!\beta_1^{i-k}\beta_2^{k-m}\beta_3^{m-p}\beta_4^{q}\beta_5^{p-q}}{(i-k)!(k-m)!(m-p)!(p-q)!q!}$$
$$\times\sum_{s=0}^{2k-m-q}\frac{(-1)^s 2^{2m-p+q+s}(2k-m-q)!}{(2k-m-q-s)!s!(\alpha_1+\sqrt{\alpha_2^2+\alpha_3^2})^{n+2i}}$$
$$\times\frac{\Gamma(w/2+s)\Gamma(w/2)}{\Gamma(w+s)}F(n+2i, w/2+s; w+s; \nu).$$

Finally, the expression for J_n is obtained as

$$J_n = \pi r\sum_{i=0}^{\infty}\frac{\left(\frac{n}{2}\right)_i\left(\frac{n}{2}+\frac{1}{2}\right)_i(2a)^{2i+1}}{i!}$$
$$\times\sum_{k=0}^{i}\sum_{m=0}^{k}\sum_{p=0}^{m}\sum_{q=0}^{p}\frac{(2k-m-q)!}{(i-k)!(k-m)!(m-p)!(p-q)!q!}$$
$$\times\sum_{s=0}^{2k-m-q}\frac{(-1)^s 2^{2m-p+q+s}}{(2k-m-q-s)!s!}\frac{\Gamma(w/2+s)\Gamma(w/2)}{\Gamma(w+s)}\times P_{nikpqs}, \tag{33}$$

where

$$P_{nikpqs} = \int_0^{\pi}\frac{\beta_1^{i-k}\beta_2^{k-m}\beta_3^{m-p}\beta_4^{q}\beta_5^{p-q}\sin^{2i+1}\gamma\sqrt{a^2\cos^2\gamma+b^2\sin^2\gamma}}{(\alpha_1+\sqrt{\alpha_2^2+\alpha_3^2})^{n+2i}}$$
$$\times F(n+2i, w/2+s; w+s; \nu)d\gamma,$$

where P_{nikpqs} needs to be evaluated numerically. Therefore, the expression for the interaction energy between a ring and an ellipsoid can be obtained by substituting J_n defined by (33) for $n = 3$ and 6 into (28).

References

1. R. Bakry, R.M. Vallant, M.N. ul Haq, M. Rainer, Z. Szabo, C.W. Huck, G.K. Bonn, Medicinal applications of fullerenes. Int. J. Nanomed. **2**, 639–649 (2007)
2. B.J. Cox, N. Thamwattana, J.M. Hill, Mechanics of atoms and fullerenes in single-walled carbon nanotubes. I. acceptance and suction energies. Proc. R. Soc. A **463**, 461–476 (2007)
3. B.J. Cox, N. Thamwattana, J.M. Hill, Mechanics of atoms and fullerenes in single-walled carbon nanotubes. II. oscillatory behaviour. Proc. R. Soc. A **463**, 477–494 (2007)
4. E. Dietel, A. Hirsch, B. Pietzak, M. Waiblinger, K. Lips, A. Weidinger, A. Gruss, K.P. Dinse, Atomic nitrogen encapsulated in fullerenes: effects of cage variations. J. Am. Chem. Soc. **121**, 2432–2437 (1999)
5. M.S. Dresselhaus, G. Dresselhaus, P.C. Eklund, *Science of Fullerenes and Carbon Nanotubes* (Academic Press, USA, 1996)
6. L.A. Girifalco, M. Hodak, R.S. Lee, Carbon nanotubes, buckyballs, ropes, and a universal graphitic potential. Phys. Rev. B **62**, 13 104–13 110 (2000)
7. B. Goeddea, M. Waiblingerb, P. Jakesa, N. Weidena, K.P. Dinsea, A. Weidingerb, 'Nitrogen doped' C_{60} dimers ($N@C_{60}$-C_{60}). Chem. Phys. Lett. **334**, 12–17 (2001)
8. W. Harneit, Fullerene-based electron-spin quantum computer. Phys. Rev. A **6**5, 032,322 (2002)
9. W. Harneit, C. Meyer, A. Weidinger, D. Suter, J. Twamley, Architectures for a spin quantum computer based on endohedral fullerenes. Phys. Status Solidi B **233**, 453–461 (2002)
10. N. Karasuma: HPLC Column for Fullerene Separation: COSMOSIL Buckyprep, COSMOSIL PBB. Nacalat Tesque, Inc., Nakagyo-ku, Kyoto 604–0855, JAPAN, http://www.nacalai.com
11. T.A. Murphy, T. Pawlik, A. Weidinger, M. Höhne, R. Alcala, J.M. Spaeth, Observation of atomlike nitrogen in nitrogen-implanted solid C_{60}. Phys. Rev. Lett. **77**, 1075–1078 (1996)
12. B. Naydenov, C. Spudat, W. Harneit, H. Süss, J. Hulliger, J. Nuss, M. Jansen, Ordered inclusion of endohedral fullerenes $N@C_{60}$ and $P@C_{60}$ in a crystalline matrix. Chem. Phys. Lett. **424**, 327–332 (2006)
13. T. Suetsuna, N. Dragoe, W. Harneit, A. Weidinger, H. Shimotani, S. Ito, H. Takagi, K. Kitazawa, Separation of $N_2@C_{60}$ and $N@C_{60}$. Chem. Eur. J. **8**, 5079–5083 (2002)
14. M. Waiblinger, K. Lips, W. Harneit, A. Weidinger, Corrected article: thermal stability of the endohedral fullerenes $N@C_{60}$, $N@C_{70}$, and $P@C_{60}$ [Phys. Rev. B 63, 045421 (2001)]. Phys. Rev. B **64**, 159,901 (2001)
15. B.C. Yadav, R. Kumar, Structure, properties and applications of fullerenes. Int. J. Nanotech. Appl. **2**, 15–24 (2008)
16. M.C. Zumwalt, M.B. Denton, Using high performance liquid chromatography to determine the C_{60} : C_{70} ratio in fullerene soot. J. Chem. Edu. **10**, 939–940 (1995)